

Design of a CPG-Based Close-Loop Direction Control System for Lateral Undulation Gait of Snake-Like Robots

Quan Minh Dao, Quan Tuong Vo

Department of Mechatronics, Faculty of Mechanical Engineering

Ho Chi Minh City University of Technology - VNU HCM

Ho Chi Minh City, Vietnam

41202963@hcmut.edu.vn, vtquan@hcmut.edu.vn

Abstract—This paper aims to propose a paradigm of constructing the system which is capable of controlling the locomotion direction of Lateral Undulation gait of snake-like robots. Firstly, we explain the function of each essential component of such system as well as their means of implementation. Secondly, we deliver a control scheme which unifies all these components to make a single complete system that helps reduce many degrees of freedom of snake-like robots to just one in the context of direction control. Finally, some simulations are conducted to verify the ability of such system. A part of which is also tested with a real robot.

Keywords—snake-like robots, head-navigated, direction control

I. INTRODUCTION

Snake-like robots were first introduced to the world in 1972 by Hirose. Since then, this type of robots has attracted great attention of researchers because of their ability of maneuvering across various environments as well as the challenge which rises when ones want to control their motion. The reason for such challenge is that snake-like robots has a highly redundant structure which results in a large number of degrees of freedom (DOFs), with at least threes being under-actuated (the pose of robot head link in global frame).

The earliest work of controlling snake-like robots is documented in [1] where Hirose used sin-wave signals as desired angular position of motors actuating revolute joints of his snake robot ACM I. Sinusoidal movements of those motors creates the rhythmic oscillation among robot joints which leads to the S-shape motion of the whole mechanism. This S-shape motion mimics the Lateral Undulation (i.e. crawling) gait of biological snakes.

The pioneer works of Hirose is based on the hypothesis that the evolution of snake muscle force must be smooth and periodic. Meanwhile, recent researches on snake-like robots [2]–[5] are inspired by the core of the nervous system of vertebrate animals the Central Pattern Generator (CPG). A single CPG has the description of either neural or nonlinear oscillator [6]. If a number of CPGs are coupled together to form a network, they can produce rhythmic signals which can be used in same manner as sin-wave.

Both sin-wave and CPG-based method are capable of creating S-shape motion in snake-like robots. However, they need to be integrated with other controllers to achieve the motion direction control. Methods for steering snake robots are summarized by Ye in [7]. All of which has been implemented in CPG-controlled snake robots [8]–[10].

A part from the advantage/disadvantage of each steering method, ones has to carefully consider the crucial question of which feature of a snake-like robot is chosen to represent the heading direction of the whole structure. To tackle that question, researchers take the inspiration from the nature where snakes point their head toward their forward direction so that the head can represent robots direction of motion. The methods to navigate the head link (i.e. the first link) are detailed in [11], [12]. Another answer is the use of the body frame named Virtual Chassis [13] which is formed by robot principle moments of inertia. Although the latter approach is less obvious, it enables every part of robots to contribute to robot global pose. Therefore, it powers a more macroscopic control.

The paragraphs above suggest that a locomotion direction control system of snake-like robots can be constructed out of three components: a CPGs network, a steering method, and an appropriate representation of motion direction. A study on such system has been carried out by Wu and Ma in [9]. Their system is the only one of this control scheme. The first component of their system CPGs network is made of Matsuoka oscillator which is categorized as a neural oscillator. The second component is the Amplitude Modulation Method (AMM) [7], and they employ head-navigated method as the last one.

In this paper, we focus on controlling locomotion direction of snake-like robots Lateral Undulation gait. To this end, we build a control system of the same type as [9], with different means of implementation. In detail, we use a nonlinear oscillator named Kuramoto oscillator [14] to make the CPGs network and Virtual Chassis to represent the movement of the whole robot. For the steering method, we keep the AMM because of their linear relationship between this method control signal and robot turning angle [7]. Despite of not using head-navigated

method to represent robot moving direction, we still propose a novel head-navigated method to benefit further the integration of cameras or sensors on robots head link. Beyond that, we demonstrate a systematic framework to analyze and control snake robots motion by dividing this problem into three subproblems, namely creating rhythmic motion among robot joints, localizing robot motion, and steering robot. By tackling one subproblem at a time in this order, we can overcome the challenges relating to many DOFs of snake-like robots by gradually reducing them into one. Furthermore, this final DOF can be directly controlled by modifying a parameter of the proposed CPGs network.

Since we only focus on the Lateral Undulation gait, the configuration of snake-like robots taken into account is the chain of $(N+1)$ identical links connected by N revolute joints which have axis perpendicular to plane of robot locomotion, like ACM I [1].

II. DESIGN OF THE CPGs NETWORK

A. Mathematical Equations and structure of the network

Taking the inspiration of CPGs networks design in [3], [5] we first use the single chain bidirectional coupling network described in Fig.1. In this figure, an arrow represents a connection which goes from the CPG at its origin to the one at its tip. The value written on the connection which is either φ or $-\varphi$ informs the phase lag between these two CPGs. The differential equations system describing the whole network is

$$\dot{\theta}_k = \begin{cases} 2\pi v + w \sin(\theta_2 - \theta_1 + \varphi), & k = 1 \\ 2\pi v + w \left[\begin{matrix} \sin(\theta_{k-1} - \theta_k - \varphi) + \\ \sin(\theta_{k+1} - \theta_k + \varphi) \end{matrix} \right], & 2 \leq k \leq N-1 \\ 2\pi v + w \sin(\theta_{N-1} - \theta_N - \varphi), & k = N \end{cases} \quad (1)$$

$$\phi_k = A \cos(\theta_k), 1 \leq k \leq N \quad (2)$$

Here, v is the intrinsic frequency parameter, while w is the coupling strength of connections in the network. These two parameters are positive and constant. $\theta_k, \dot{\theta}_k, \phi_k$ are respectively the state variable, its first-order time derivative, and the output of the k^{th} CPG in the network of N CPGs. ϕ_k is then used as reference signal of angular position of snake robot k^{th} joint. A is the amplitude of oscillation.

As mention in section I, the S-shape motion of snake-like robots is created by rhythmic oscillation among robot joints i.e. every joint oscillates with the same frequency and constant phase shift. In other words, the system of (1) and (2) must

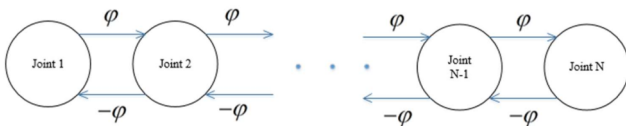


Fig. 1. Single chain bidirectional coupling CPGs network

converge to its limit cycle [15]. To prove this, assign $(\theta_{k+1} - \theta_k + \varphi)$ to χ_k and rewrite (1) as

$$\dot{\chi}_k = \begin{cases} -2ws_1 + ws_2, & k = 1 \\ ws_{k-1} - 2ws_k + ws_{k+1}, & 2 \leq k \leq N-2 \\ ws_{N-2} - 2ws_{N-1}, & k = N-1 \end{cases} \quad (3)$$

In (3) and all the equations below, s_k is the abbreviation of $\sin(\chi_k)$. $\dot{\chi}_k$ is the first-order time derivative of χ_k , so $\dot{\chi}_k = \dot{\theta}_{k+1} - \dot{\theta}_k$. The convergence of (1) and (2) is directly defined by the convergence of $\chi = [\chi_1 \ \chi_2 \ \dots \ \chi_{N-1}]^T$ to the origin of $\mathbb{R}^{(N-1) \times 1}$. Use the following at Lyapunov candidate function

$$L(\chi) = (N-1) - \sum_{k=1}^{N-1} \cos(\chi_k) \quad (4)$$

The positive definite of $L(\chi)$ is trivial. Take the first-order time derivative of (4)

$$\dot{L}(\chi) = \sum_{k=1}^{N-1} \dot{\chi}_k s_k \quad (5)$$

Substituting (3) to 5 yields

$$\dot{L}(\chi) = -2w \left(\sum_{k=1}^{N-1} s_k^2 - \sum_{k=2}^{N-1} s_{k-1} s_k \right) \quad (6)$$

The Cauchy inequality $(a^2 + b^2)/2 \geq ab$ with any real a, b ensures that

$$\dot{L}(\chi) \leq 0, \forall \chi \in \mathbb{R}^{(N-1) \times 1} \quad (7)$$

The equality in (7) happens if and only if $\chi = 0^{(N-1) \times 1}$ that means $\dot{L}(\chi)$ is semi-negative definite. Therefore, $L(\chi)$ has been proved to be a Lyapunov function leading to the asymptotically stability of $\mathbb{R}^{(N-1) \times 1}$ origin. For this reason, the system of (1) and (2) converges to its limit cycle.

B. Head-navigated CPGs Network

As prior explanation, despite of not being used to describe the moving direction of the whole robot, the navigated head link can benefit further application of snake-like robots, especially those evolves with cameras or sensors mounted on robots head. To realize this, we modify the network structure in Fig.1 to form the one in Fig.2. The observation of the locomotion with a single S-shape formed by the whole robot indicates that if the first link moves in an reverse-phase manner relative to the third link, the net displacement of the first link is approximately parallel to the direction of locomotion.

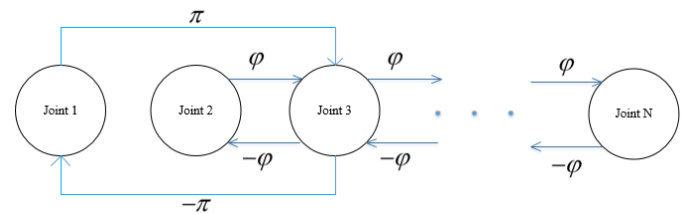


Fig. 2. Head-navigated CPGs Network

That observation results in the modified structure displayed in Fig.2. The system of equation describing this network and its convergence can be deduced in the same manner as the single chain bidirectional coupling network.

The simulation as well as experiment results presented latter will verify the effectiveness of our CPGs network structure.

III. CONTROL OF LOCOMOTION DIRECTION

A. Steering method - Amplitude Modulation Method (AMM)

The AMM is integrated into the two CPGs network above to the steer the crawling motion of snake-like robots by modifying (2) as the following

$$\phi_k = A[1 + \Delta \text{sign}(\cos \theta_k)] \cos \theta_k \quad (8)$$

In (8), ΔA plays the role of control signal thanks to its linear time invariant (LTI) relationship robot turning angle. The detail proof of this relationship is provided in [9].

B. The Virtual Chassis

The Virtual Chassis is a local frame having its origin attached to robot center of mass (COM). Its axes aligned with robot principal moments of inertia. The idea of this frame is to isolate the robot internal deformation caused by joints movement from the net displacement of the whole mechanism in the global frame [13] which is the same function as a car chassis, hence its name.

Placing a local frame at the COM of each link which is assumed to be coincident with link middle point as in Fig.3. In this figure, every joint is at their zero position. $O_k x_k y_k (k = 1, N+1)$ is the local frame attached to the k^{th} link. $J_h (h = 1, N)$ denotes the h^{th} joint connecting h^{th} link and $(h+1)^{th}$ link. $O^g x^g y^g$ is the global frame. To compute the coordinate of Virtual Chassis axes with respect to an initial body frame says the one attached on the first link, one needs to construct the following matrix P

$$P = \begin{bmatrix} x_1^1 - \bar{x}^1 & y_1^1 - \bar{y}^1 \\ \vdots & \vdots \\ x_{N+1}^1 - \bar{x}^1 & y_{N+1}^1 - \bar{y}^1 \end{bmatrix} \quad (9)$$

In (9) and the following equations, the superscripts denote the reference frames. (x_k^1, y_k^1) , (\bar{x}^1, \bar{y}^1) are respectively co-ordinates of the origin of k^{th} local frame and coordinates of robot COM, relatively to the frame at the first link. The coordinates of Virtual Chassis axes in two-dimension space are

the eigenvectors of matrix $P^T P$ [13]. They are put together to form matrix $V \in \mathbb{R}^{2 \times 2}$, with each axis being a column.

To construct matrix P , coordinates of the origin of k^{th} frame relative to the first one can be computed through homogeneous transformation.

$$T_k^1 = T_2^1 T_3^2 \dots T_k^{k-1}, 2 \leq k \leq N+1 \quad (10)$$

The third column of matrix T_k^1 is coordinates of the origin of k^{th} frame relative to $O_1 x_1 y_1$ written in the homogeneous form. Matrix T_k^{k-1} expresses the pose of k^{th} frame with respect to $k-1^{th}$ and is computed by

$$T_k^{k-1} = \begin{bmatrix} \cos \phi_{k-1} & -\sin \phi_{k-1} & -d(1 + \cos \phi_{k-1}) \\ \sin \phi_{k-1} & \cos \phi_{k-1} & -d \sin \phi_{k-1} \\ 0 & 0 & 1 \end{bmatrix} \quad (11)$$

The parameter d in (11) is the distance from O_k to J_{k-1} which is a half of link length. The pose of Virtual Chassis with respect to the first link frame is introduced as (12)

$$T_{VC}^1 = \begin{bmatrix} V & (\bar{x}^1, \bar{y}^1)^T \\ 0^{1 \times 2} & 1 \end{bmatrix} \quad (12)$$

To be ready to use as sensory feedback for locomotion direction controller, the pose of Virtual Chassis is expressed in the global frame as

$$T_{VC}^g = T_{VC}^1 T_1^g \quad (13)$$

In (13), T_1^g is the homogeneous transformation representing the pose of first link frame in global frame which can only be obtained by measuring the coordinate of the first link position and direction in global frame. The robot direction of locomotion is the first column of T_{VC}^g .

At this point, we have delivered all of the three components making up the control system described in section I. The next subsection shows how to unify them.

C. Control Scheme

To control the direction of Lateral Undulation gait of snakelike robots, the CPGs network, the AMM, and the Virtual Chassis are interconnected in the control scheme as illustrated in Fig.4. In this figure, γ_d, γ_{VC} are the desired and robot actual direction of locomotion, respectively. The Direction Controller is realized by a proportional controller thanks to the LTI relationship between direction control input, ΔA , and robot turning angle.

$$\Delta A = K_P(\gamma_{VC} - \gamma_d) \quad (14)$$

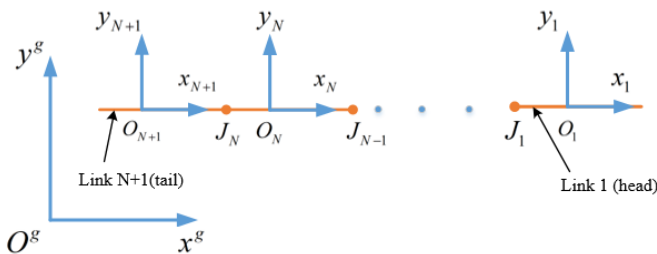


Fig. 3. Local frame attached to each link

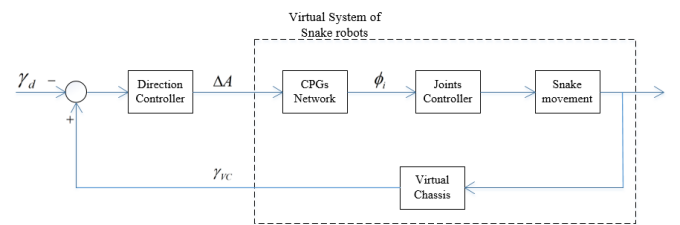


Fig. 4. Control scheme for controlling the direction of crawling motion

The combination of CPGs network, the AMM, and Virtual Chassis as in Fig.4 simplifies the many DOFs of snake robots to a single one which is γ_{VC} in the context of direction control of crawling motion. Together those three can be considered as a virtual SISO system representing snake-like robots.

IV. SIMULATION RESULTS

To validate the effectiveness of our proposed method, we conduct some simulations based on the V-REP software with ODE being chosen as the physic engine. The simulation model takes the same intrinsic geometry and control parameters of our real robots listed in the Table.I.

TABLE I
MODEL PARAMETERS

Parameter	Value
Link length	0.2 (m)
Wheel friction coefficient	0.035
Link weight	0.23 (kg)
Number of joints (N)	7
CPG frequency (v)	0.5 (Hz)
Coupling strength (w)	15
Phase lag (φ)	$2\pi/7$ (rad)
CPG oscillation amplitude (A)	$\pi/9$ (rad)
Direction controller parameter (K_P)	0.75

A. Head Navigation

The body shape of our model of snake-like robot produced by the single chain bidirectional coupling CPGs network (Fig.1) is shown in Fig.5. Obviously, the whole robot forms a complete S-shape which means the head link, i.e. L_1 , points away from the moving direction. In contrast, the application of head-navigated network (Fig.2) results in a relatively parallel between the first link and the moving direction which is illustrated in Fig.6. These visual results will be latter backed up by quantity analysis.

B. Maintaining a Straight Forward Motion

The problem happens to snake-like robots while they perform crawling (i.e. lateral undulating) gait is the normal direction slippery which has been investigated in [16]. This

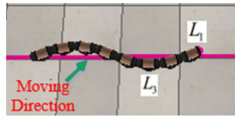


Fig. 5. Robot body shape generated by single chain bidirectional coupling network

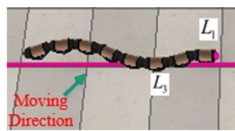


Fig. 6. Robot body shape generated by head-navigated network

is why we employ the maintaining a straight forward motion as the first test for our direction control scheme (Fig.4).

The result of this test with the initial condition of y-coordinate of robot COM being 0 is displayed in Fig.7 and Fig.8. They show that the single chain network delivers smaller maximum error, with the fluctuation of robot COM y-coordinate being significantly higher than head-navigated network. This is because robot controlled by head-navigated network experiences a more severe side slippery effect. This is evidenced in the way biological snakes crawl where they slightly lift their head off the ground. Furthermore, since the first link of robot controlled by head-navigated network nearly does not move relatively to the moving direction. Therefore, the number of links contributing to the fluctuation of robot COM reduces by one, hence a less aggressive fluctuation.

The effect of head-navigated network on the direction of the first link is clarified by Fig.9 and Fig.10. While the data in the former describes a large difference between head link direction and moving direction, the latter indicates a small difference in the amplitude as well as phase between these two directions.

V. EXPERIMENTAL RESULTS

The experiments in this section are conducted on our snake-like robot prototype. This robot employs Tiva TM4C123G launchpad as its controller unit. This board collects the value of the angle γ_{head} which is measured by the compass sensor HMC5883L mounted on robot head and transmits it to a laptop. Here, γ_{head} is used to compute the reference angular positions of robot joints, $\phi_i (i = 1, N)$ by going through the control scheme in Fig.4. The laptop then transmits ϕ_i back to robot control unit to regulates the position of RC Servo motors actuating robot joints.

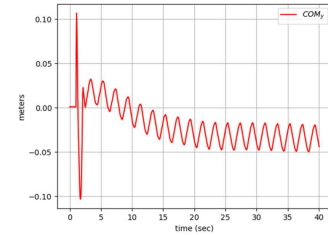


Fig. 7. The variation of y-coordinate of robot COM controlled by single chain bidirectional coupling network

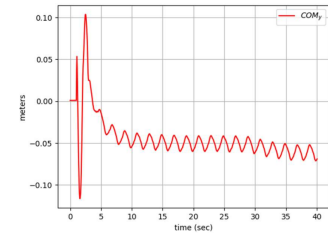


Fig. 8. The variation of y-coordinate of robot COM controlled by head-navigated network

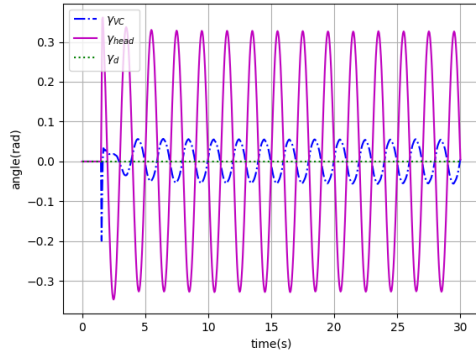


Fig. 9. The variation of head link direction (γ_{head}) compared to direction of the whole robot (γ_{VC}) controlled by single chain network

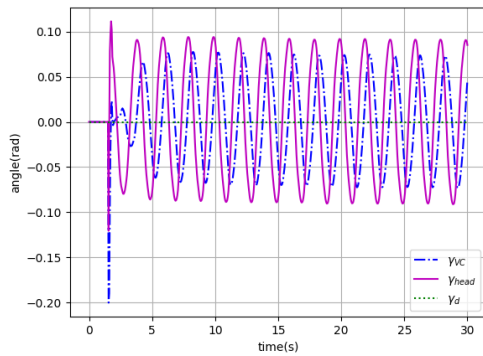


Fig. 10. The variation of head link direction (γ_{head}) compared to direction of the whole robot (γ_{VC}) controlled by head-navigated network

A. Head Navigation

The body shape of our real robot controlled by two networks is captured in Fig.11 and Fig.12. In these figures, the head link is the one being closest to the bottom of pictures. It is noticeable that the head-navigated CPGs network can keep the head link pointing toward robot moving direction (Fig.12).

B. Maintaining a Straight Forward Motion

This experiment is carried out to show that the direction control scheme proposed in this paper can steer the real robot to negotiate the side slipping effect. It can be seen from Fig.13

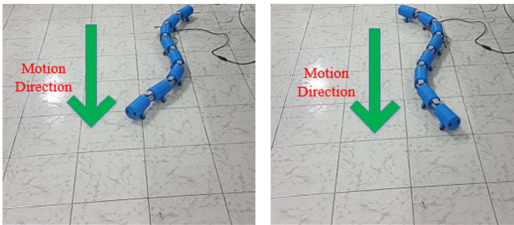


Fig. 11. The body shape of real robot controlled by the single chain network

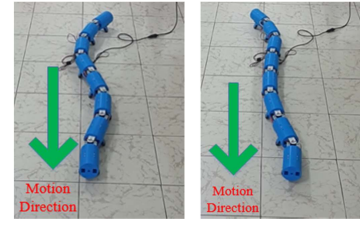


Fig. 12. The body shape of real robot controlled by the head-navigated network

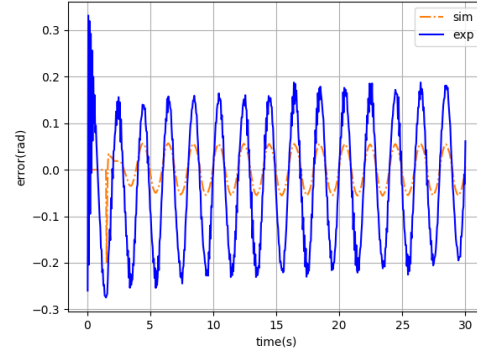


Fig. 13. Forward direction error of robot controlled by the single chain network

and Fig.14 that the integration of the direction control into either single chain or head-navigated CPGs network results in the stable oscillation of robot direction error, ($\gamma_{VC} - \gamma_d$) around 0.

In contrast to the match of error profile between experiment (the continuous line) and simulation (the dash line) results of the head-navigated network, the error in experiment with the single chain network oscillates with a significant larger amplitude, compared to the simulation. We have found that the compass sensor is affected non-uniform amplitude of the magnet field in the experiment room. For this reason, in

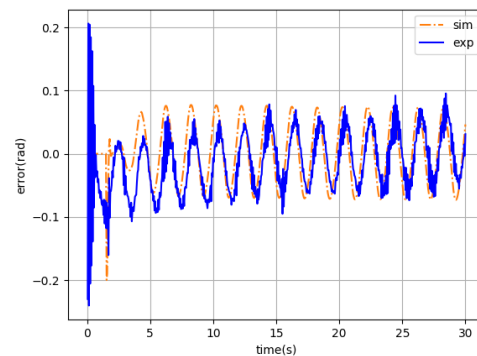


Fig. 14. Forward direction error of robot controlled by the head-navigated network

the experiment with the single chain network, the first link oscillation (with respect to robot motion direction) make the sensor measurement oscillate with a large amplitude, hence the gap between experiment and simulation results.

C. Turning Motion

The last two figures illustrate the evolution of robot direction error, $(\gamma_{VC} - \gamma_d)$, when robot make a turn of $-\pi/12$ (rad), away the initial forward direction. In this experiment, the turning signal is generated by the change of γ_d from 0 to $-\pi/12$. To prevent the jerky movement of robot joints, this change is made as a linear function and lasts within 2 seconds from $time = 3(s)$. The results displayed in Fig.15 and Fig.16 share the features of the results of the previous experiment.

VI. CONCLUSIONS

To sum up, this paper propose a locomotion direction control system for the Lateral Undulation (i.e. crawling) gait of snake-like robots. This system is made up with three components: the CPGs Network, the steering method AMM, and the Virtual Chassis. The significance of such system is its ability of reducing the many DOFs of snake-like robots to a single one in problems relating to the control of locomotion direction. The simulations and experimental results verify this ability as well as the effectiveness of the proposed system.

However, we have not managed to limit noise exerting on our robot compass sensor. In addition, the use of RC Servo motors leads to the lack of feedback information of actual robot joints angular position. Although this limitation does not significantly affect our results, it rises the concern that there might be difference between actual joints position and CPGs network output signals.

In the next steps, we will work on two weaknesses above, and then continue to control other gaits of snake-like robots as well as optimize them in the term of energy consumption and locomotion speed.

ACKNOWLEDGMENT

This research is funded by Viet Nam National University Ho Chi Minh City (VNU-HCM) under Grant number C2016-20-33.

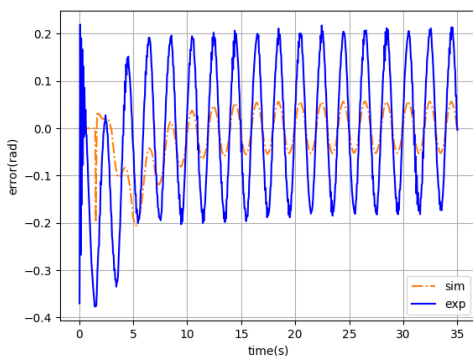


Fig. 15. Turning error of robot controlled by the single chain network

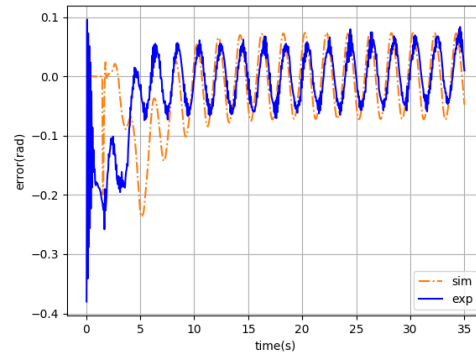


Fig. 16. Turning error of robot controlled by the head-navigated network

REFERENCES

- [1] S. Hirose, *Biologically Inspired Robots: Snake-Like Locomotors and Manipulators*. Oxford University Press, 1995, vol. 48, no. 3.
- [2] A. Crespi, A. Badertscher, A. Guignard, and A. J. Ijspeert, "AmphiBot I: An amphibious snake-like robot," *Robotics and Autonomous Systems*, vol. 50, no. 4, pp. 163–175, 2005.
- [3] A. Crespi, A. J. A. Ijspeert, and E. P. F., "AmphiBot II : An Amphibious Snake Robot that Crawls and Swims using a Central Pattern Generator," ... *Conference on Climbing and Walking Robots* (...), no. September, pp. 19–27, 2006.
- [4] X. Wu and S. Ma, "CPG-based Control of Serpentine Locomotion of a Snake-like Robot," *IFAC Proceedings Volumes*, vol. 42, no. 16, pp. 705–710, 2009.
- [5] N. M. Nor and S. Ma, "A simplified CPGs network with phase oscillator model for locomotion control of a snake-like robot," *Journal of Intelligent and Robotic Systems: Theory and Applications*, vol. 75, no. 1, pp. 71–86, 2014.
- [6] J. Yu, M. Tan, J. Chen, and J. Zhang, "A survey on CPG-inspired control models and system implementation," *IEEE Transactions on Neural Networks and Learning Systems*, vol. 25, no. 3, pp. 441–456, 2014.
- [7] Changlong Ye, Shugen Ma, Bin Li, and Yuechao Wang, "Turning and side motion of snake-like robot," in *IEEE International Conference on Robotics and Automation, 2004. Proceedings. ICRA '04. 2004*, vol. 5, no. January. IEEE, 2004, pp. 5075–5080.
- [8] A. J. Ijspeert and A. Crespi, "Online trajectory generation in an amphibious snake robot using a lamprey-like central pattern generator model," in *Proceedings 2007 IEEE International Conference on Robotics and Automation*. IEEE, apr 2007, pp. 262–268.
- [9] X. Wu and S. Ma, "Neurally controlled steering for collision-free behavior of a snake robot," *IEEE Transactions on Control Systems Technology*, vol. 21, no. 6, pp. 2443–2449, 2013.
- [10] N. M. Nor and S. Ma, "CPG-based locomotion control of a snake-like robot for obstacle avoidance," in *2014 IEEE International Conference on Robotics and Automation (ICRA)*. IEEE, may 2014, pp. 347–352.
- [11] H. Yamada, M. Mori, and S. Hirose, "Stabilization of the head of an undulating snake-like robot," in *2007 IEEE/RSJ International Conference on Intelligent Robots and Systems*. IEEE, oct 2007, pp. 3566–3571.
- [12] Xiaodong Wu and Shugen Ma, "Head-navigated locomotion of a snake-like robot for its autonomous obstacle avoidance," in *2010 IEEE/RSJ International Conference on Intelligent Robots and Systems*, vol. 1, no. c. IEEE, oct 2010, pp. 401–406.
- [13] D. Rollinson, A. Buchan, and H. Choset, "Virtual chassis for snake robots: Definition and applications," *Advanced Robotics*, vol. 26, no. 17, pp. 1–22, 2012.
- [14] J. A. Acebrón, L. L. Bonilla, C. J. P. Vicente, F. Ritort, and R. Spigler, "The Kuramoto model: A simple paradigm for synchronization phenomena," *Reviews of Modern Physics*, vol. 77, no. 1, pp. 137–185, 2005.
- [15] E. Izhikevich and Y. Kuramoto, "Weakly coupled oscillators," *Encyclopedia of mathematical physics*, vol. 5, p. 448, 2006.
- [16] Shugen, "Analysis of creeping locomotion of a snake-like robot," *Advanced Robotics*, vol. 15, no. 2, pp. 205–224, jan 2001.